Fits to NC high-x data and measurement of charm production in CC

A. Solano
Univ. of Torino and INFN
on behalf of ZEUS Collaboration

Outline:

A − Analysis of ZEUS neutral current high-x data with Transfer Matrix
[ZEUS-prel-18-002; ZEUS Coll., Phys. Rev. D89 (2014) 072007]

B − Measurement of charm production in charged current with ZEUS data
[ZEUS-prel-18-004]

DifLowx 2018, Reggio Calabria

HERA and the ZEUS detector

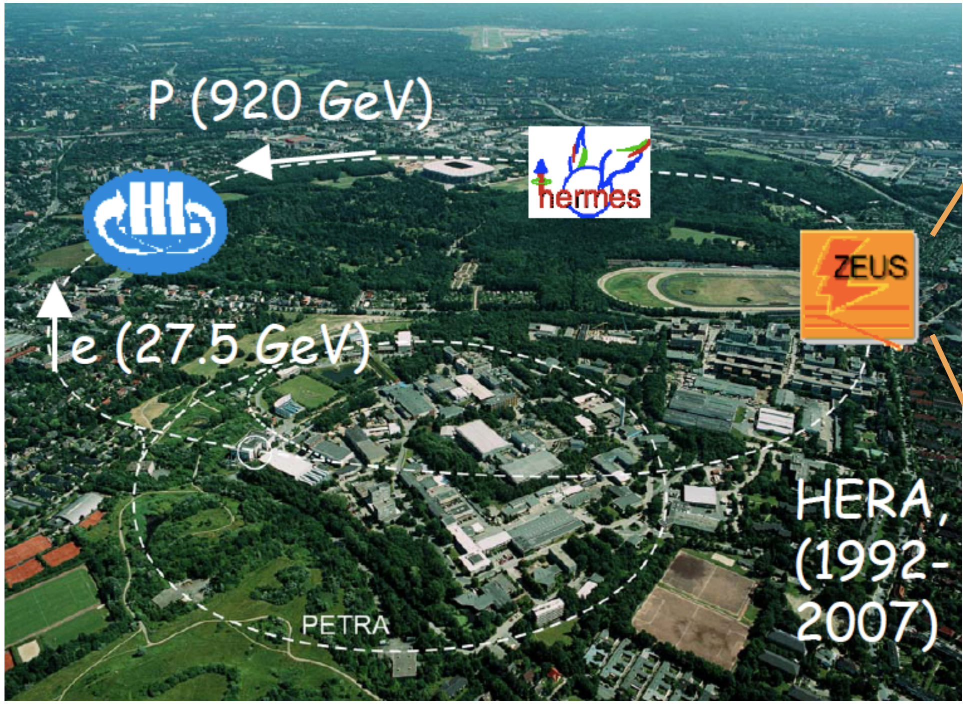

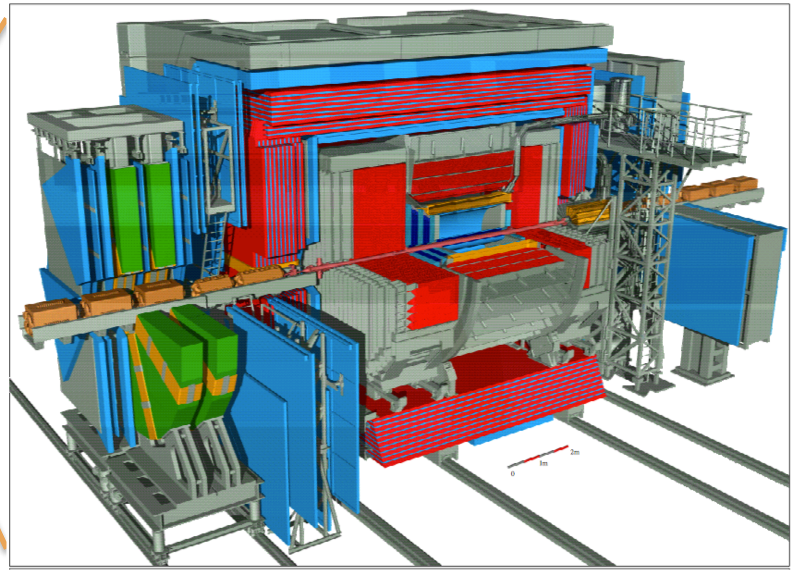

ZEUS detector, asymmetric with extended coverage in the proton beam direction

HERA-II : 2001-2007

p : 920 GeV $\quad e^+/e^-$: 27.5 GeV

575 GeV

460 GeV

Most of the collected data are at $\sqrt{s}$ = 318 GeV
Analyses presented here use these data

A – Motivation of studying published high-x data

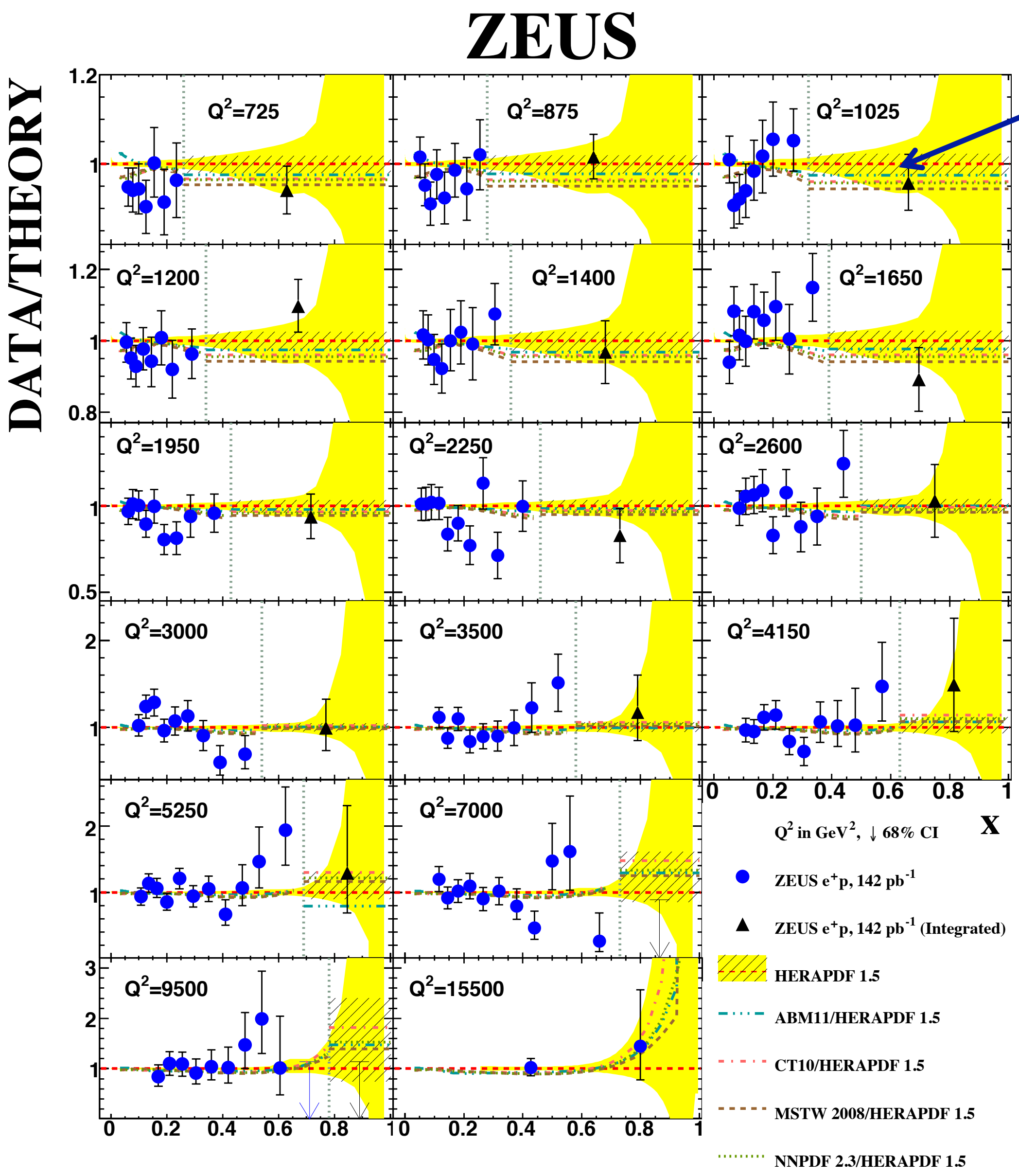

Integrated bins
(cross sections integrated in x)

Largest-x ZEUS data not yet used in the extraction of PDFs

Note the uncertainty bands above x~0.65, high-x data can impact here

Despite the small number of events, significant information on the behaviour of the PFDs at high-x can be extracted from the data

The analysis aims at **comparing the predictions for the expected number of events from the different PDF sets to the number observed by ZEUS** using Poisson statistics, **drawing conclusions based on the level of agreement**

A – Transfer Matrix for the ZEUS detector

A **Transfer Matrix** for the detector has been developed, using which the **number of events reconstructed in data can be predicted from any PDF** as below:

- get a prediction for the generator/hadron level number of events in true bin i, which is luminosity x radiative corrections x Born cross section

$$\nu_{i,k} = \mathcal{L} K_{ii} \sigma_{i,k}$$

- apply transfer matrix element a_{ij} to get the number of events in a bin j

$$\nu_{j,k} \approx \sum_i a_{ij} \nu_{i,k}$$

L : data luminosity
K_{ii} : radiative corrections (calculated using HERACLES)
$\sigma_{i,k}$: Born level cross sections in i^{th} bin for k^{th} PDF

a_{ij} has all detector and analysis effects
(probability of an event reconstructed in j^{th} bin to come from i^{th} true bin)

Elements K_{ii} and a_{ij} are taken to be independent of the PDF set used

A – Predicting the expectations

N = T M

||

Trasfer Matrix

(153 x 429)

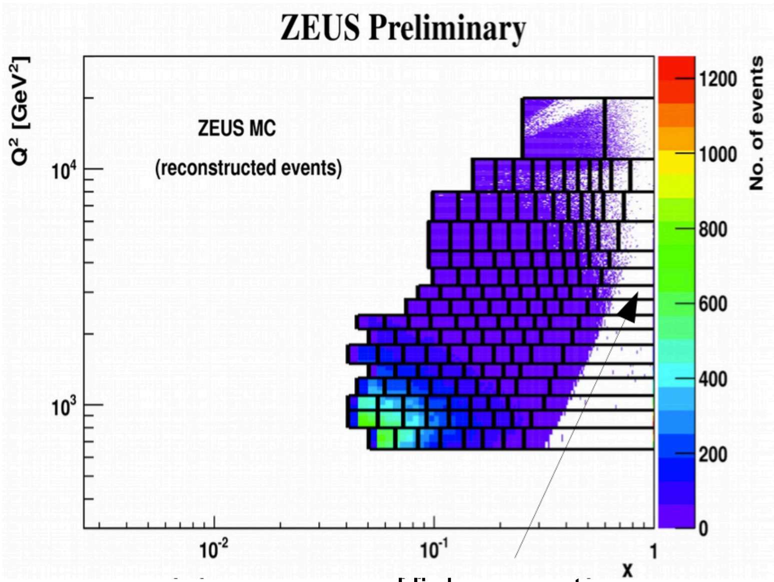

High-x events
in integrated bins

Predicted (reconstructed) x-Q²
events in **cross section binning**
(153 elements in **N** vector
= number of cross section bins)

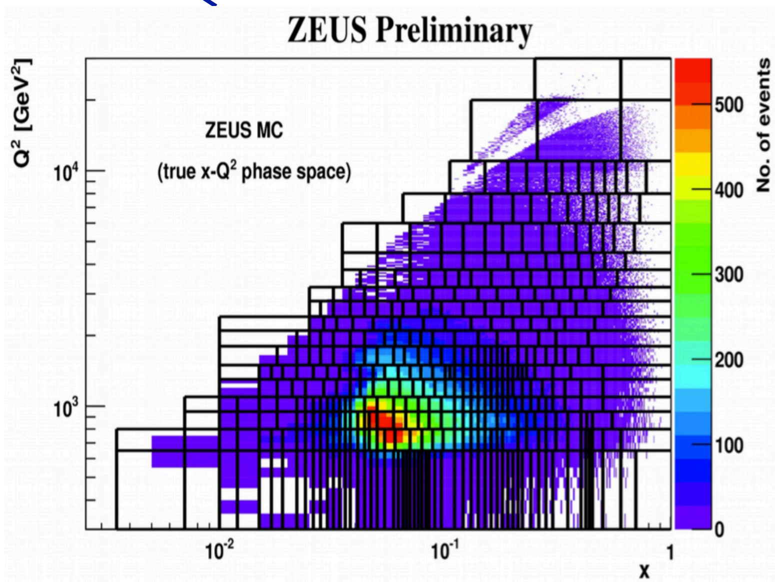

Generated x-Q² events in
extended binning
(429 elements in **M** vector
= number of generated bins)

Transfer Matrix T evaluated using
HERACLES with HERAPDF2.0

A – Comparison of different PDFs

Comparison of M from different PDFs:

Ratio of generated level cross sections from various NLO PDFs to HERAPDF2.0NLO

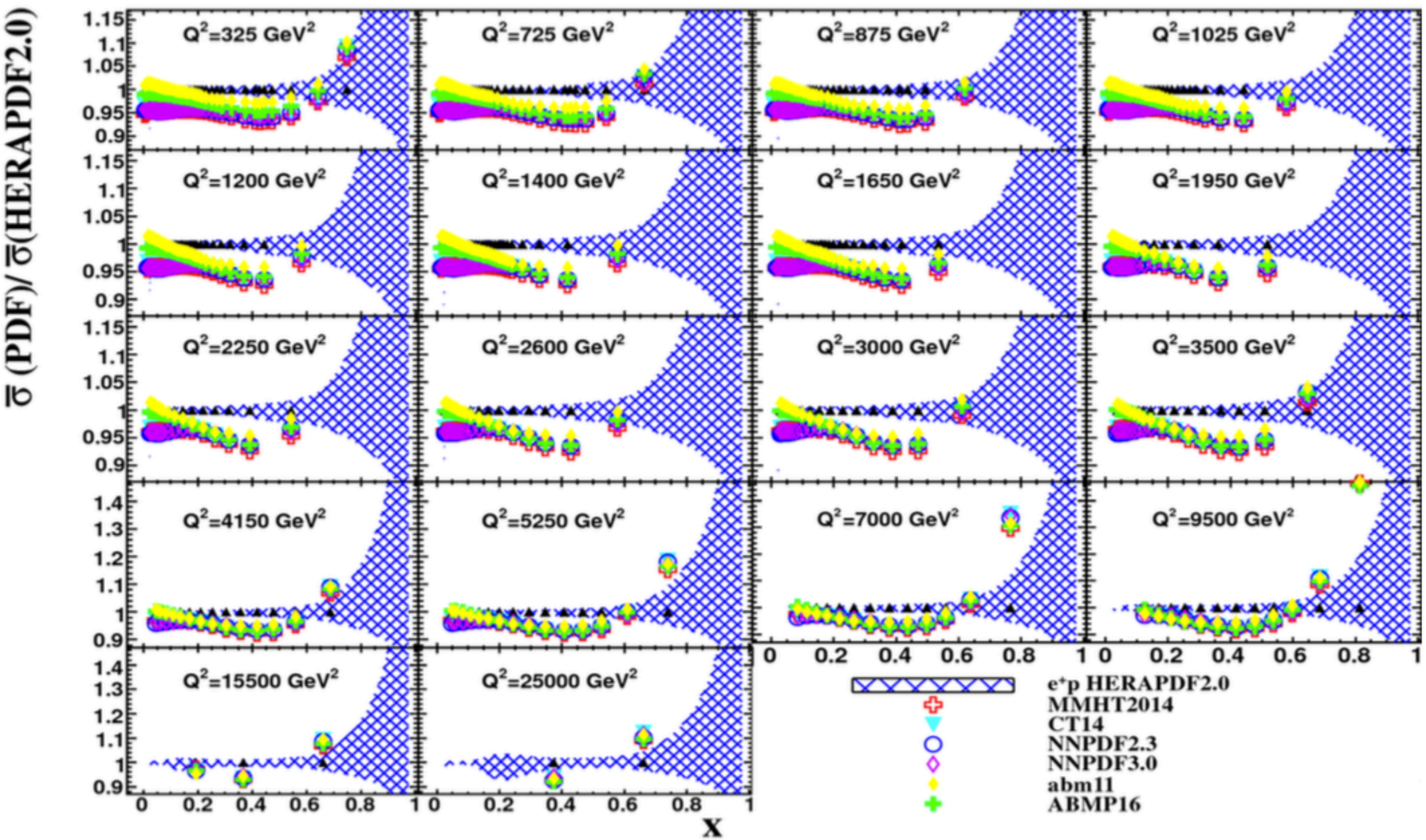

e^+p

$\overline{\sigma}$ is the total integrated cross section in a given x-Q^2 bin

Shape difference between HERAPDF and other PDFs, approaches 10% at x~0.4

A – Comparison PDF vs ZEUS data

Comparison of predicted N from PDF with number of events from data:

Ratio of number of events in data to HERAPDF2.0NLO
and 1,2,3 sigma bands from Poisson statistics

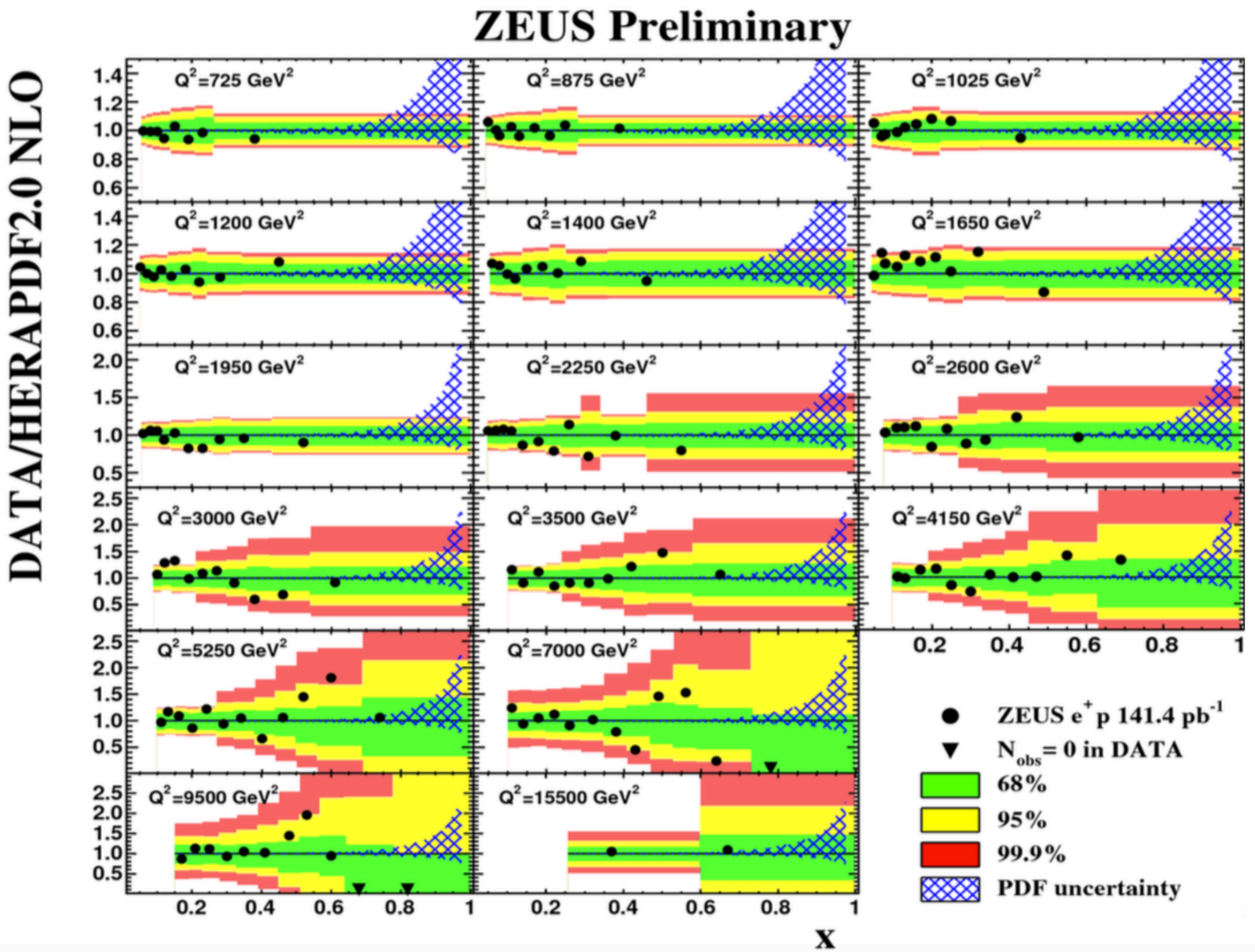

e^+p

A – Comparison PDF vs ZEUS data

Comparison of predicted N from PDF with number of events from data:

Ratio of number of events in data to HERAPDF2.0NLO
and 1,2,3 sigma bands from Poisson statistics

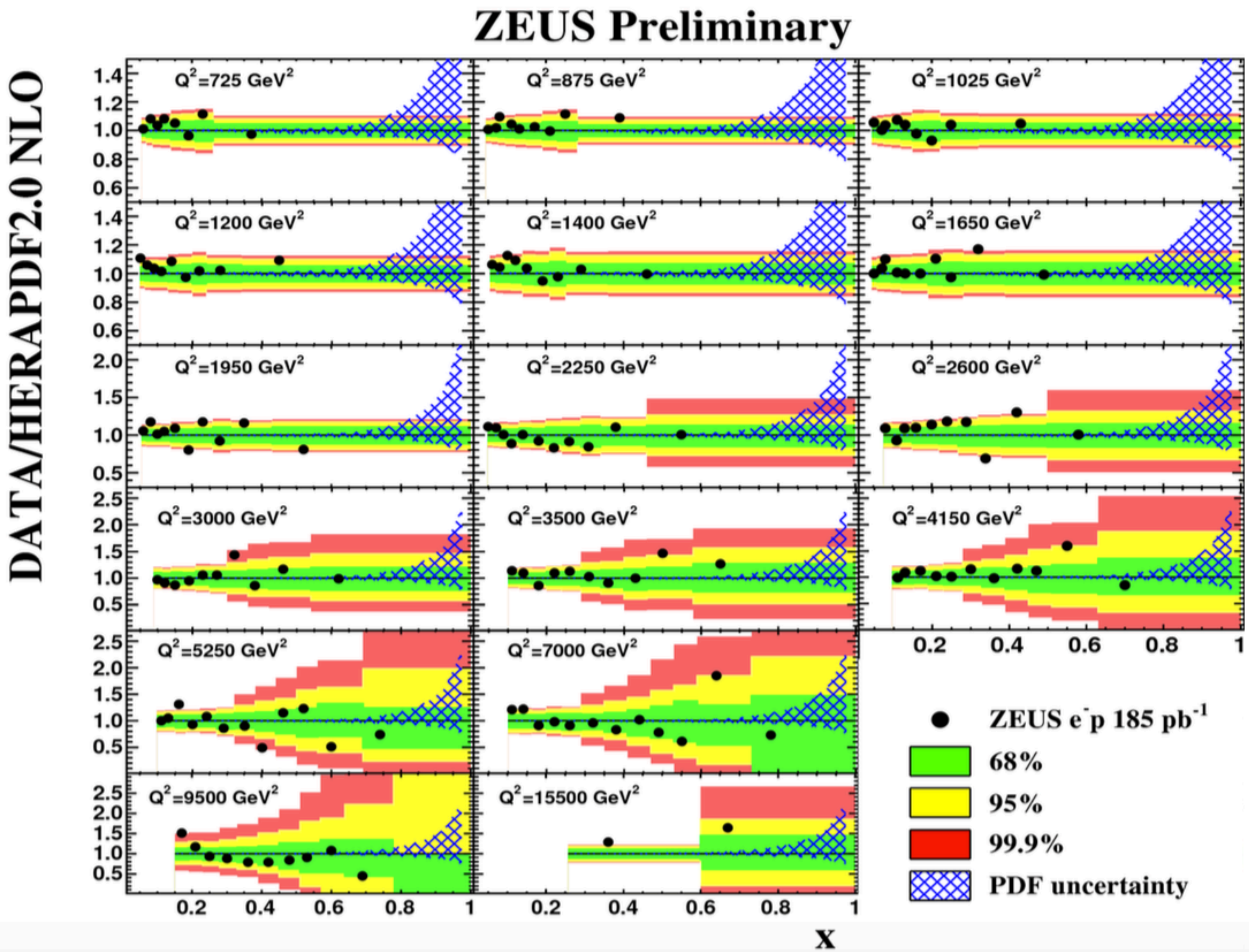

e^-p

A – Probability for explaining high-x data from different PDFs

p-values are determined from different PDFs, for the e^+p and e^-p data sets:

PDF	e^-p	e^+p
$HERAPDF2.0$	0.05	0.5
$CT14$	0.002	0.8
$MMHT2014$	0.002	0.8
$NNPDF2.3$	0.00007	0.6
$NNPDF3.0$	0.0002	0.7
$ABMP16$	0.01	0.8
$ABM11$	0.001	0.6

Only statistical fluctuations from Poisson probabilities are included

p-value from HERAPDF2.0 lower than that from other PDFs for e^+p

Much worse for e^-p

A – Probability for explaining high-x data from different PDFs in different x ranges

	e^-p		e^+p	
PDF	$x < 0.6$	$x \geq 0.6$	$x < 0.6$	$x \geq 0.6$
HERAPDF2.0	0.06	0.2	0.6	0.1
CT14	0.0008	0.2	0.7	0.6
MMHT2014	0.00003	0.1	0.6	0.6
NNPDF2.3	0.00007	0.2	0.6	0.6
NNPDF3.0	0.00003	0.2	0.6	0.6
ABMP16	0.01	0.2	0.8	0.5
ABM11	0.03	0.3	0.7	0.4

Disagreement comes primarily from low-x range in e^-p

Study of systematic uncertainties is under way

Dominant systematics is the error in normalization of data, due to the luminosity error of ±1.8%

A – Summary

- Despite the small number of events, the ZEUS high-x data can help in understanding the behaviour of PFDs at high-x

- The Transfer Matrix technique has been presented:
  it can be used to predict expected number of MC events in given cross section bins by different PDFs and then compare to the observed number of events in data

- p-values from different PDFs have been calculated and compared on the basis of their explanation of the ZEUS high-x data using the Transfer Matrix
  -- Differences are seen for different PDFs
  -- Differences are also there for e^-p and e^+p data sets and the high- and low-x ranges

Prescription on how to include high-x data in PDF fits will be provided soon

B − Motivation of studying charm in CC DIS

Charm cross section measurement in high-Q^2 charge current DIS may help in **constraining strange parton density $s(x,Q^2)$**

Complementary measurement to previous analyses at low-Q^2:

→CCFR/NuTeV : $\frac{\int_0^1 dx[xs+x\bar{s}]}{\int_0^1 dx[x\bar{u}+x\bar{d}]} = 0.477^{+0.063}_{-0.053}$ $(Q^2 = 4\,GeV^2)$ [Z. Phys. C65 (1995) 189]

→ATLAS : $\frac{s+\bar{s}}{\bar{u}+\bar{d}} = 1.13 \pm 0.05$ $(Q^2 = 1.9\,GeV^2, x = 0.023)$ [Eur. Phys. J. C77 (2017) 267]

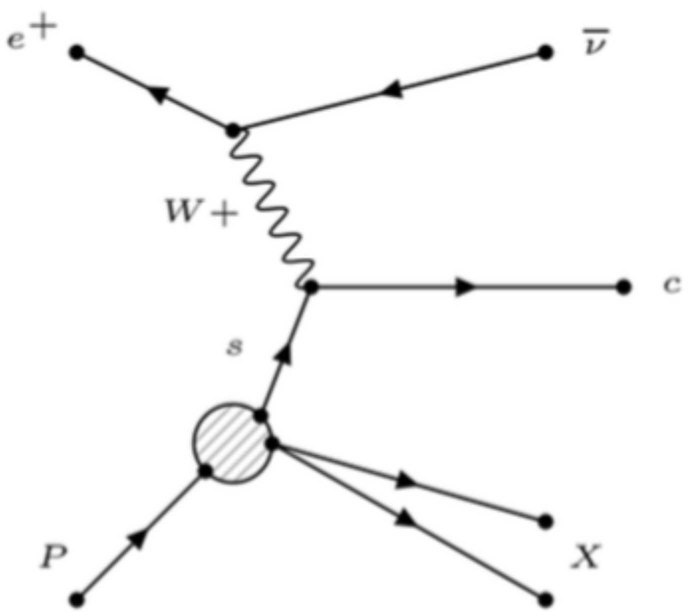

LO charm production Feynman diagram:

- Allows for $s(x,Q^2)$ measurement
- The process via the down quark is also possible but Cabibbo-suppressed
- Charmed particles have long lifetime since they decay weakly
- Due to the final state neutrino, a large missing p_T is expected

B – Samples and event selection

Data: HERA II: $L(e^+p) = 173\ pb^{-1}$; $L(e^-p) = 185\ pb^{-1}$

MC : Signal: Inclusive CCDIS - DJANGOH 1.6, ARIADNE 4.12, CTEQ5D
Background: Inclusive NCDIS - DJANGOH 1.6, ARIADNE 4.12, CTEQ5D
Photoproduction MC: HERWIG, direct and resolved

DIS event selection:

Kinematic variables defined by using the hadronic final state (JB method):

$$y_{JB} = \frac{\Sigma_h (E - p_z)_h}{2E_{e,beam}} \qquad Q^2_{JB} = \frac{p^2_{T,h}}{1 - y_{JB}} \qquad x_{JB} = \frac{Q^2_{JB}}{s y_{JB}}$$

Kinematic selection: $200\ GeV^2 < Q^2 < 60000\ GeV^2$; $y_{JB} < 0.9$

CC selection: $p_T > 12$ GeV missing transverse momentum $p_{T,miss} = p_T$
$p_T' > 10$ GeV $p_T' = p_T$ excluding CAL cells adjacent to the beam hole

Further background rejection (NC, Photoproduction, etc.)

→ ~ 4000 CC events in e^+p data and ~ 9000 in e^-p data

B – Control plots, e⁻p

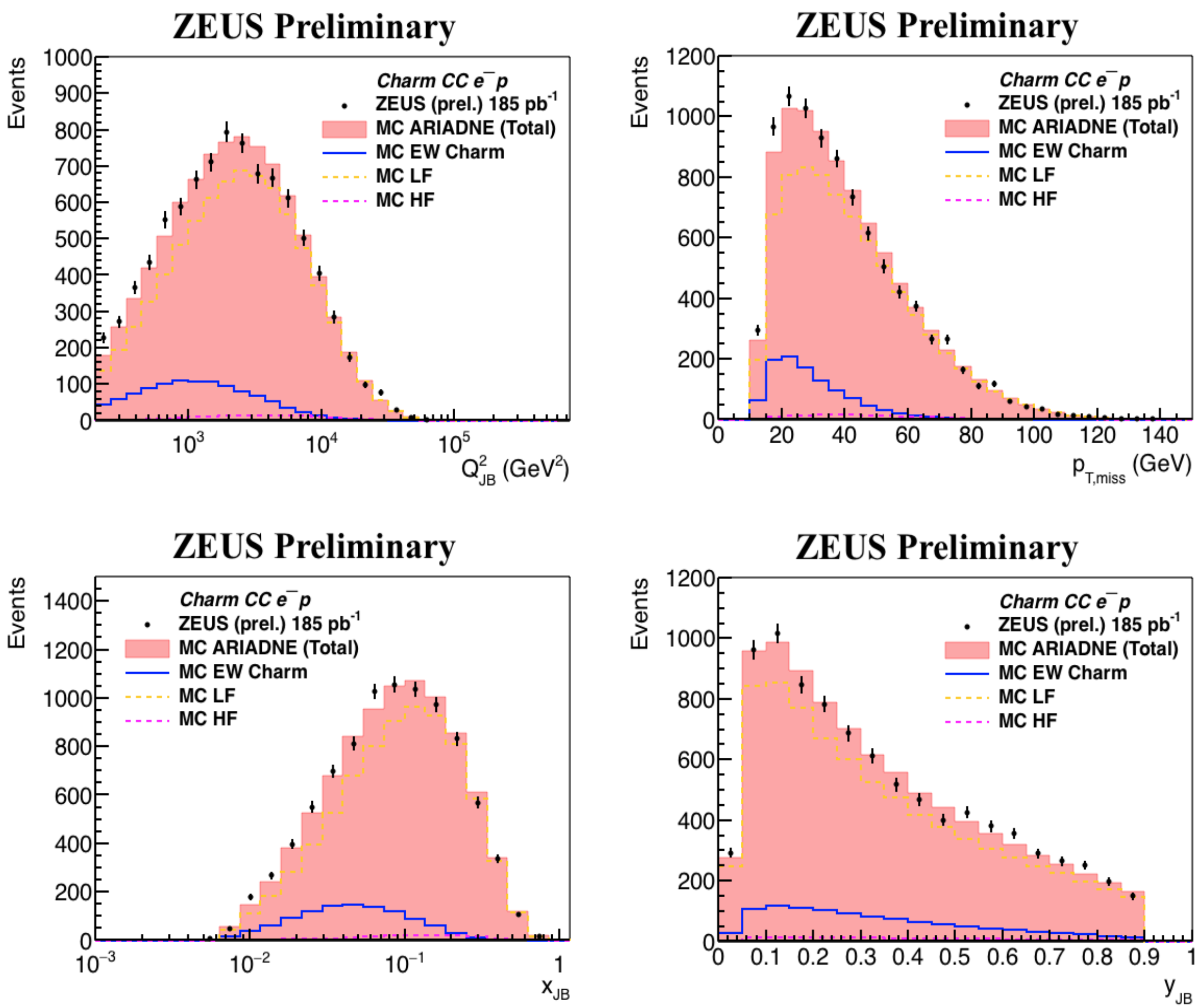

MC:

- EW Charm/Anticharm

  Charm from electroweak reaction either in the initial or final state.

- LF

  Light-flavor contribution. Major source of background

- HF

  Heavy Flavor events that do not involve EW charm

LF higher in e⁻ periods due to W-coupling valence quarks

Good consistency between data and MC

EW charm content: ~25% in e⁺p
~15% in e⁻p

B – Charm identification

The **lifetime-tagging method** is used to distinguish charmed vertices from light-flavor (LF) vertices (major source of background)

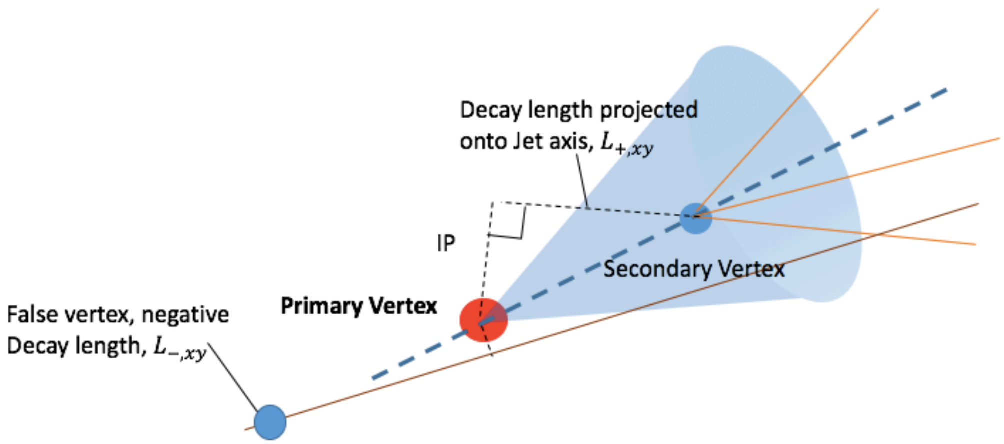

Due to the short lifetime and the finite resolution of the vertex detector, the **decay length distribution of LF vertices is symmetric, whereas that of charmed vertices is asymmetric**

Jet Selection	Reconstructed by using kT algorithm in massive mode.
	$E_T^{jet} > 5\ GeV$
	$-2.5 < \eta^{jet} < 2.5$
SecVtx Selection	$\chi^2/N_{dof} < 6$
	$\lvert Z_{secvtx} \rvert < 30\ cm$
	Distance to beamspot $\sqrt{\Delta x^2 + \Delta y^2} < 1\ cm$

${E_T}^{jet}$ and η^{jet} cuts further define the kinematic phase space of the measurement

→ Mirroring the negative decay length distribution onto the positive, the LF contribution is suppressed

B – Decay length plots

e+p

e-p

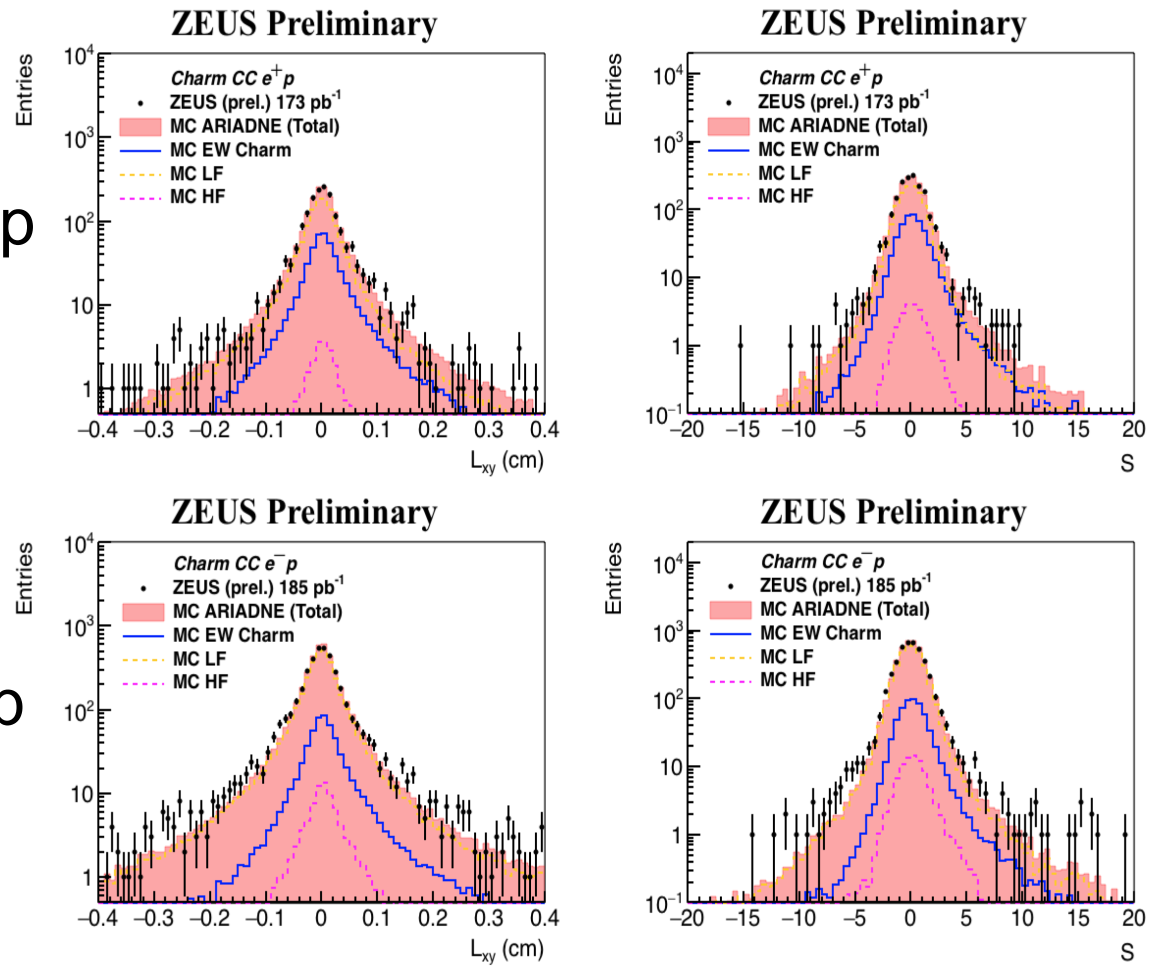

The high symmetry and large statistics around significance S~0 contributes to a large statistical uncertainty in the low bin regions in S

↓

A threshold cut on the significance is applied to reduce overall statistical uncertainty

Asymmetric charm signal can be observed

B – Mirrored decay lengths

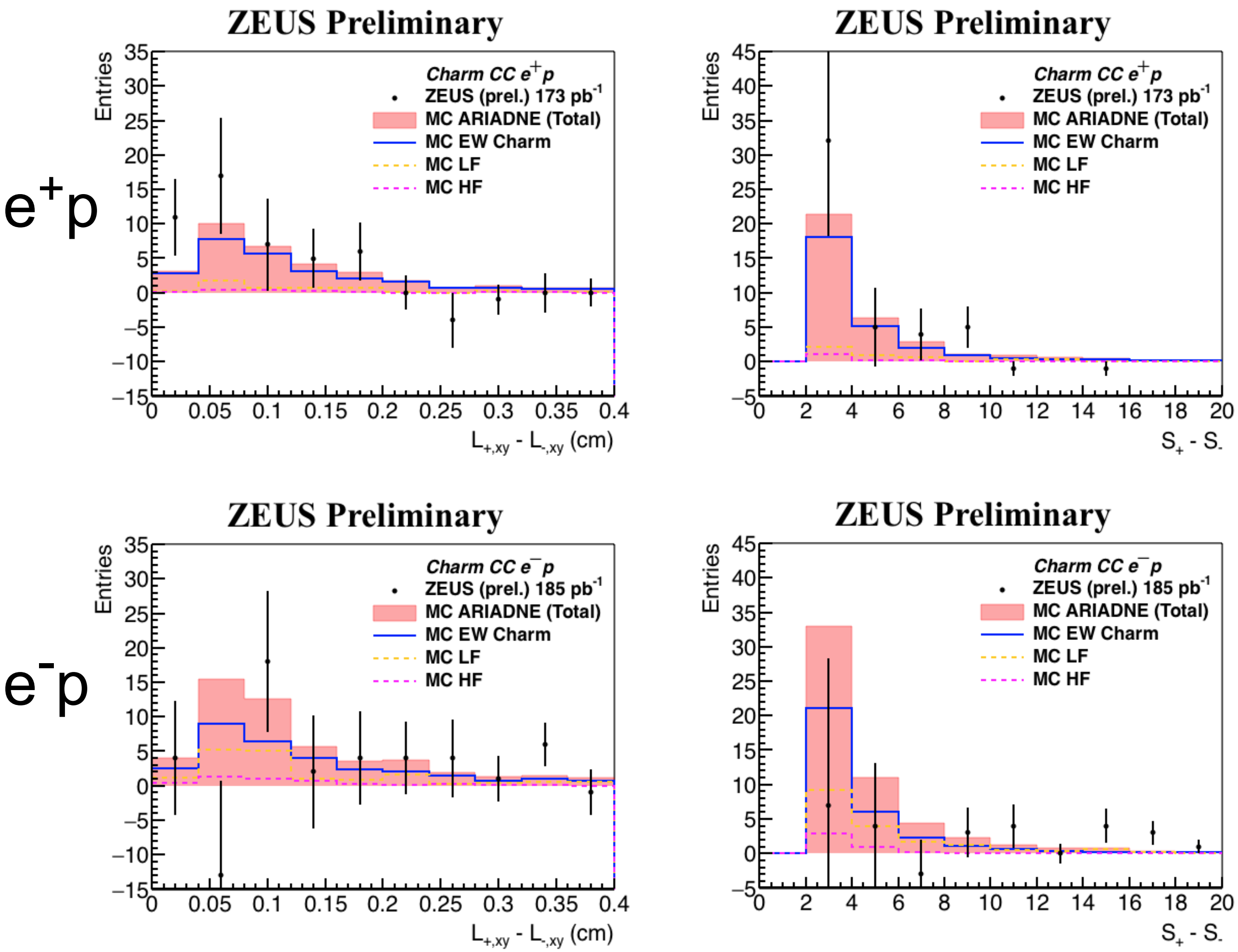

Due to their higher LF contribution, negatively-charged collisions suffer larger statistical uncertainties as well as LF background

Charm signal is extracted

Events are split into 2 bins in Q^2 to unfold the charm production cross section

B – Results

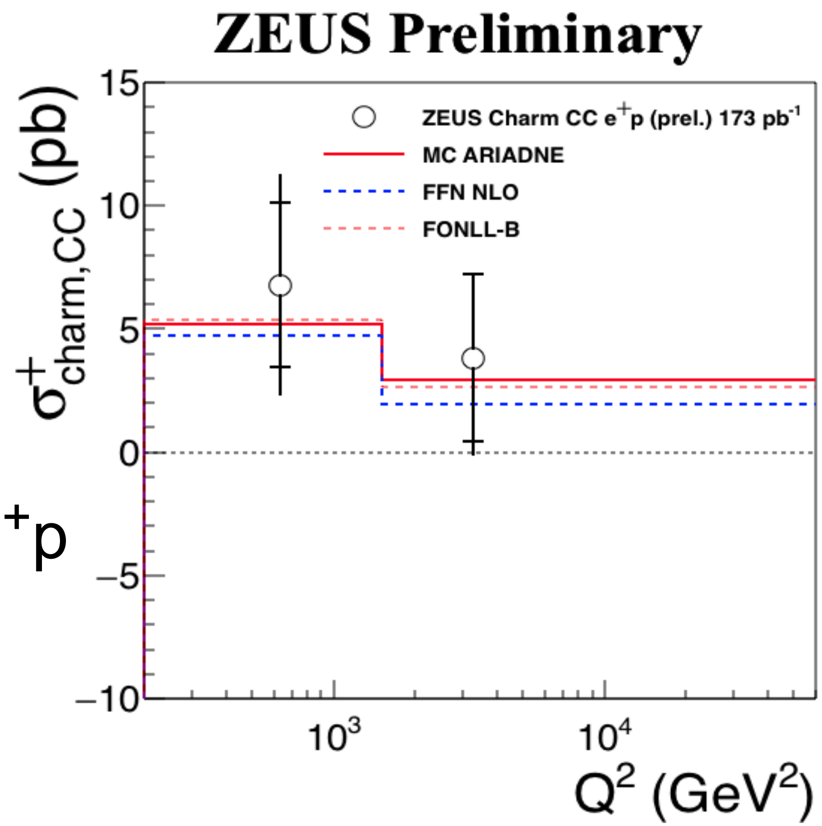

e^+p

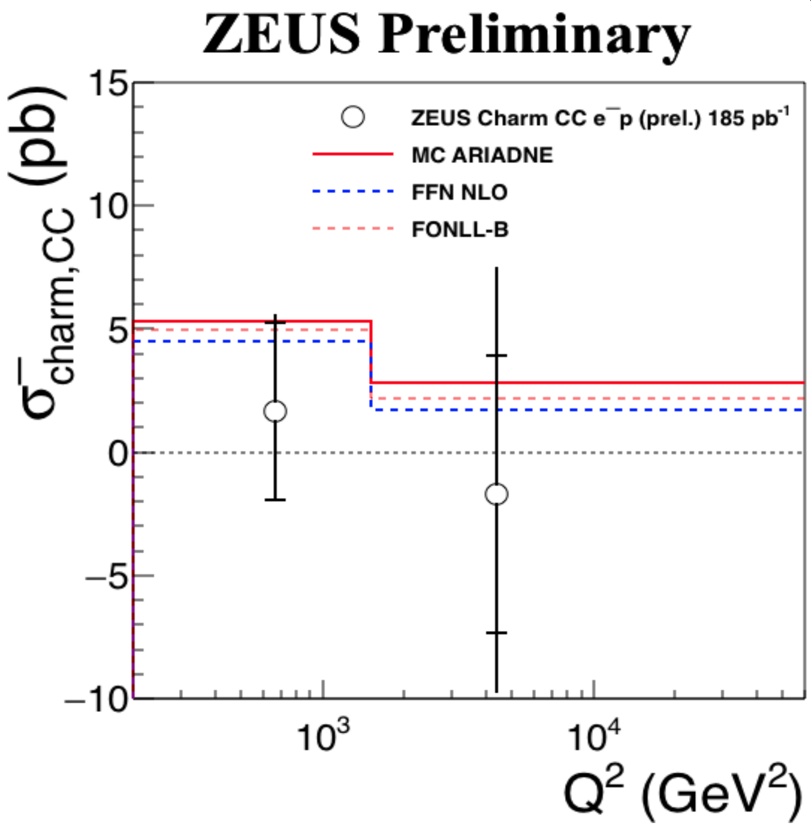

e^-p

- **Reasonable agreement between data, MC & theory with a large uncertainty**
- **MC & theory predictions suggest that the contributions from QI and BGF processes are about equal**

Theory predictions

- FFN NLO:
  ABMP16.3 NLO PDF set, OPENQCDRAD
- FONLL scheme:
  NNPDF31 NLO PDF set, APFEL

B – Summary

- Measurement of charm cross sections in the kinematic region $Q^2 > 200\ GeV^2$, y <0.9, ${E_T}^{jet} > 5\ GeV$, η^{jet} < 2.5 has been performed with the ZEUS detector using HERA II data
- Charm production cross section is 30-50% sensitive to the strange quark content of the proton, as suggested by MC and theoretical calculations (FFN NLO, FONLL-B)
- Further signal optimization to suppress LF content, especially in $e-$ periods, is in progress

This analysis shows that, with orders of magnitude higher instant luminosity and better vertex detection resolution as in the future EIC, the strange quark content of the proton could be measured via charm production in CC DIS

Backup slides

A – Comparison of different PDFs

Comparison of M from different PDFs:

Ratio of generated level cross sections from various NLO PDFs to HERAPDF2.0NLO

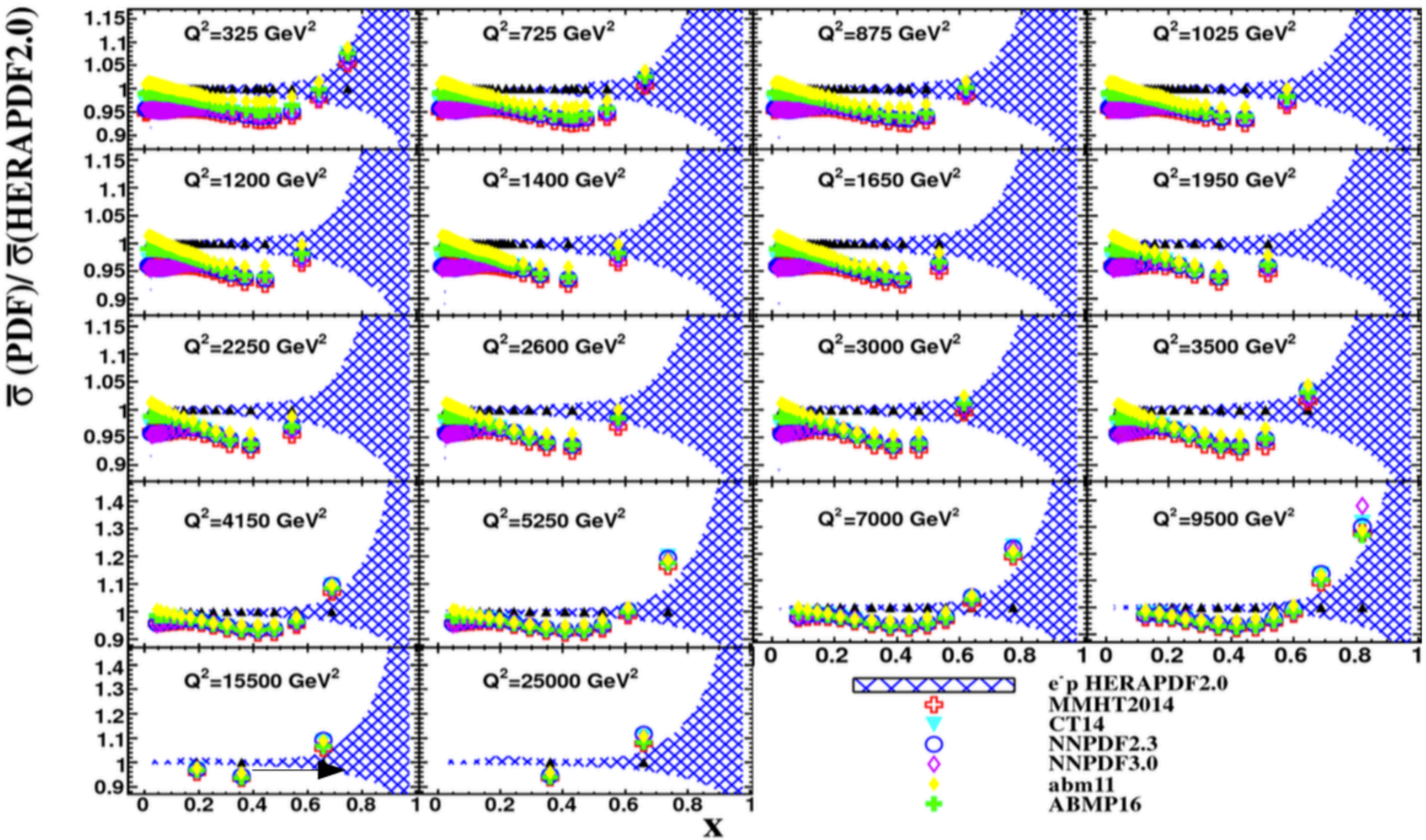

$e^{-}p$

$\bar{\sigma}$ is the total integrated cross section in a given x-Q^2 bin

Shape difference between HERAPDF and other PDFs, approaches 10% at x~0.4

A − Comparison of different PDFs

Comparison of M from different PDFs:

Ratio of generated level cross sections from various NNLO PDFs to HERAPDF2.0NNLO

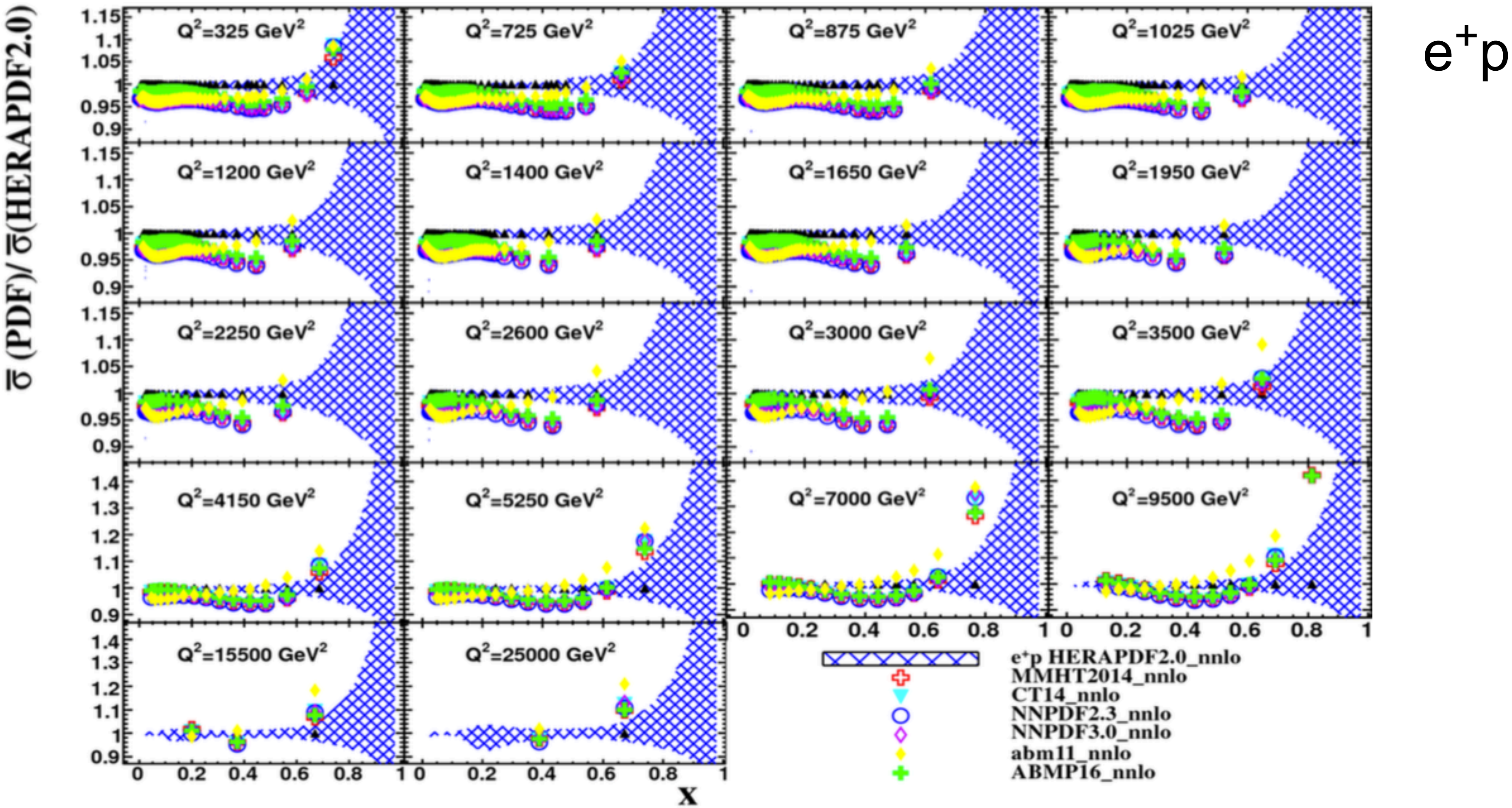

$\overline{\sigma}$ is the total integrated cross section in a given x-Q^2 bin

Shape difference between HERAPDF and other PDFs, approaches 7% at x~0.4

A – Comparison of different PDFs

Comparison of M from different PDFs:

Ratio of generated level cross sections from various NNLO PDFs to HERAPDF2.0NNLO

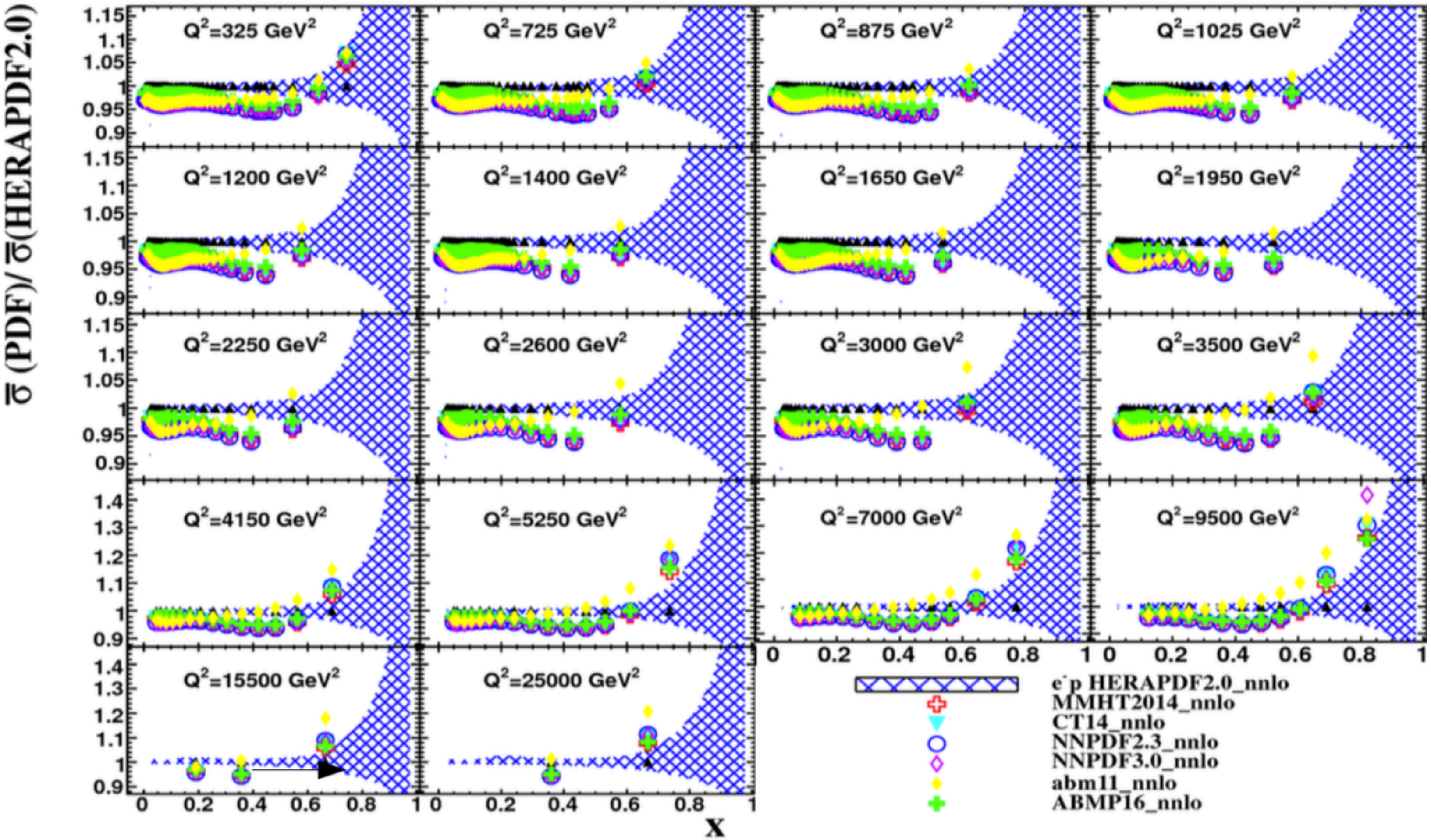

e^-p

$\bar{\sigma}$ is the total integrated cross section in a given x-Q^2 bin

Shape difference between HERAPDF and other PDFs, approaches 7% at x~0.4

A – p-value determination

Total probability for each PDF : $$P(D|M_k) = \prod_j \frac{e^{-\nu_{j,k}} \nu_{j,k}^{n_j}}{n_j!}$$

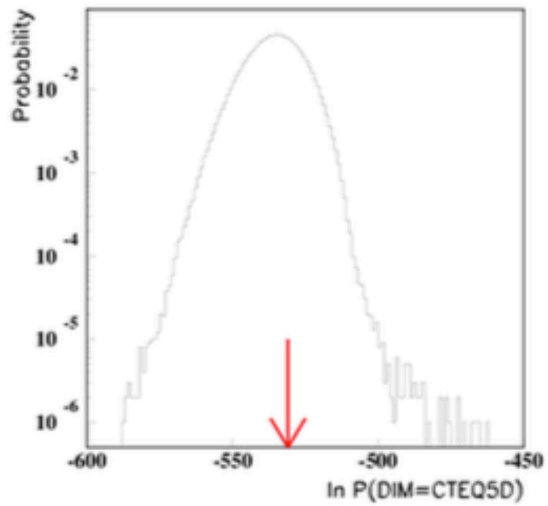

p-value is calculated by integrating out the probability from the left edge till red arrow for the given PDF

A – Systematic uncertainties

Type of Systematic Uncertainties :

I) Affecting the predictions at generator level (M values)
II) Affecting the Transfer Matrix T

Type I :

1) Luminosity uncertainty scaling M values

Type II :

1) MC statistical fluctuations (uncorrelated uncertainty)
2) All correlated and uncorrelated systematic uncertainties as in high-x paper
3) Choice of PDF for building T

A – Systematics: normalization error

Vary generated events by 1.8% up and down and calculate new p-values

+1.8 %				
	e^-p		e^+p	
PDF	$x < 0.6$	$x \geq 0.6$	$x < 0.6$	$x \geq 0.6$
HERAPDF2.0	0.02	0.1	0.2	0.3
CT14	0.02	0.3	0.8	0.5
MMHT2014	0.008	0.2	0.8	0.5
NNPDF2.3	0.009	0.3	0.8	0.4
NNPDF3.0	0.008	0.3	0.8	0.4
ABMP16	0.04	0.3	0.6	0.4
ABM11	0.03	0.3	0.4	0.2
−1.8 %				
	e^-p		e^+p	
PDF	$x < 0.6$	$x \geq 0.6$	$x < 0.6$	$x \geq 0.6$
HERAPDF2.0	0.03	0.3	0.8	0.2
CT14	0.0	0.08	0.4	0.6
MMHT2014	0.0	0.04	0.2	0.6
NNPDF2.3	0.0	0.08	0.2	0.6
NNPDF3.0	0.0	0.08	0.2	0.6
ABMP16	0.0003	0.1	0.7	0.6
ABM11	0.004	0.2	0.7	0.5

(Scale M by 1.8% up)

	e^-p		e^+p	
PDF	$x < 0.6$	$x \geq 0.6$	$x < 0.6$	$x \geq 0.6$
HERAPDF2.0	0.06	0.2	0.6	0.1
CT14	0.0008	0.2	0.7	0.6
MMHT2014	0.00003	0.1	0.6	0.6
NNPDF2.3	0.00007	0.2	0.6	0.6
NNPDF3.0	0.00003	0.2	0.6	0.6
ABMP16	0.01	0.2	0.8	0.5
ABM11	0.03	0.3	0.7	0.4

(Scale M by 1.8% down)

Dominant systematics : due to error in normalization of data quoted as 1.8 %

B – Charm production processes in CC DIS

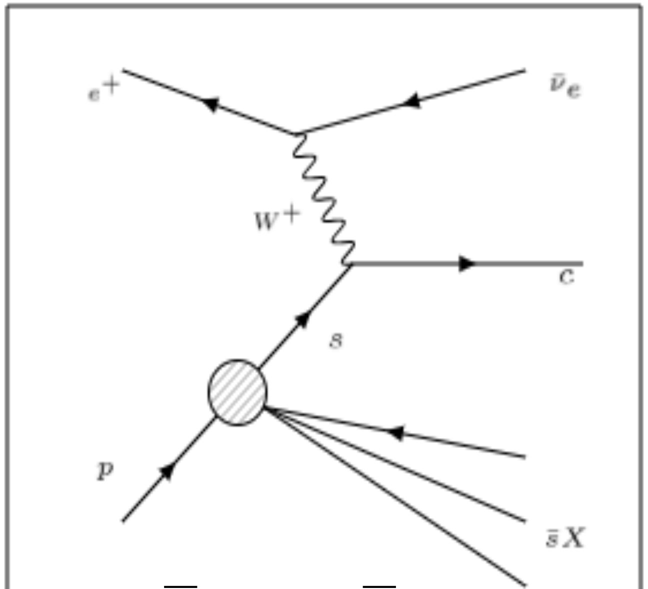

$s\bar{s}\,(d) \rightarrow c\bar{s}\,(d)$

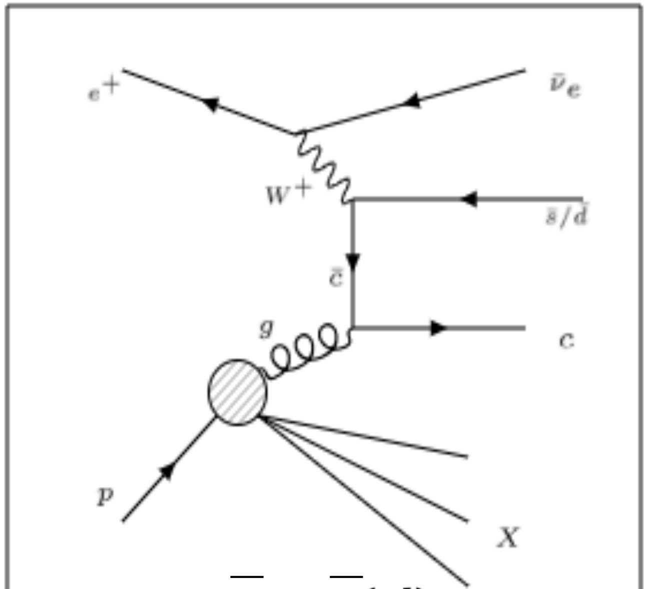

$g \rightarrow c\bar{c} \rightarrow c\bar{s}\,(d)$

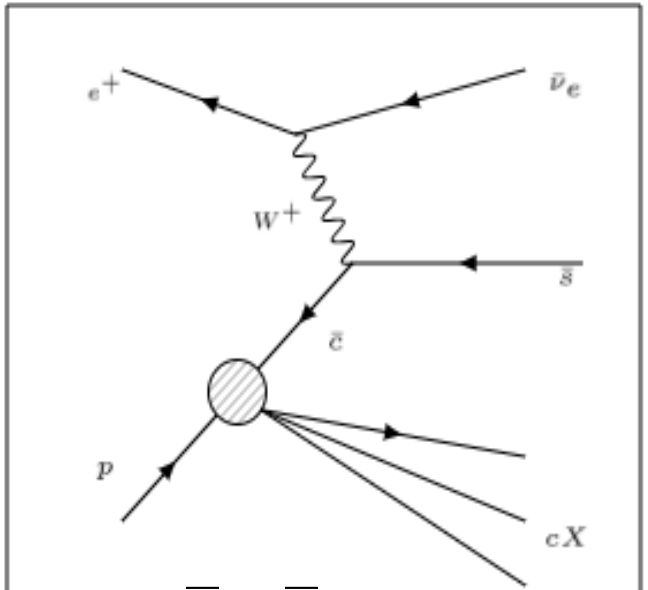

$c\bar{c} \rightarrow c\bar{s}\,(d)$

LO quark-initiated process (QI)
sensitive to strange content

NLO boson-gluon fusion (BGF)
sensitive to gluon content

LO, strange production
sensitive to charm content

Same initial and final state → hard to disentangle

B – Charm production in CC

- Charged current events are always weak interactions.

$$\frac{d^2\sigma_{Born}^{CC,e^\pm p}}{dxdQ^2} = (1 \pm P_e)\frac{G_F^2}{4\pi x}\left(\frac{M_W^2}{M_W^2 + Q^2}\right)^2 \tilde{\sigma}_{CC}^{e^\pm p}$$

- The double-differential cross section is sensitive to different quark densities.

$$\tilde{\sigma}_{CC}^{e^+p} = x[\bar{u} + \bar{c} + (1-y)^2(d + \boldsymbol{s})]$$
$$\tilde{\sigma}_{CC}^{e^-p} = x[u + c + (1-y)^2(\bar{d} + \bar{\boldsymbol{s}})]$$

B – Control plots, e^+p

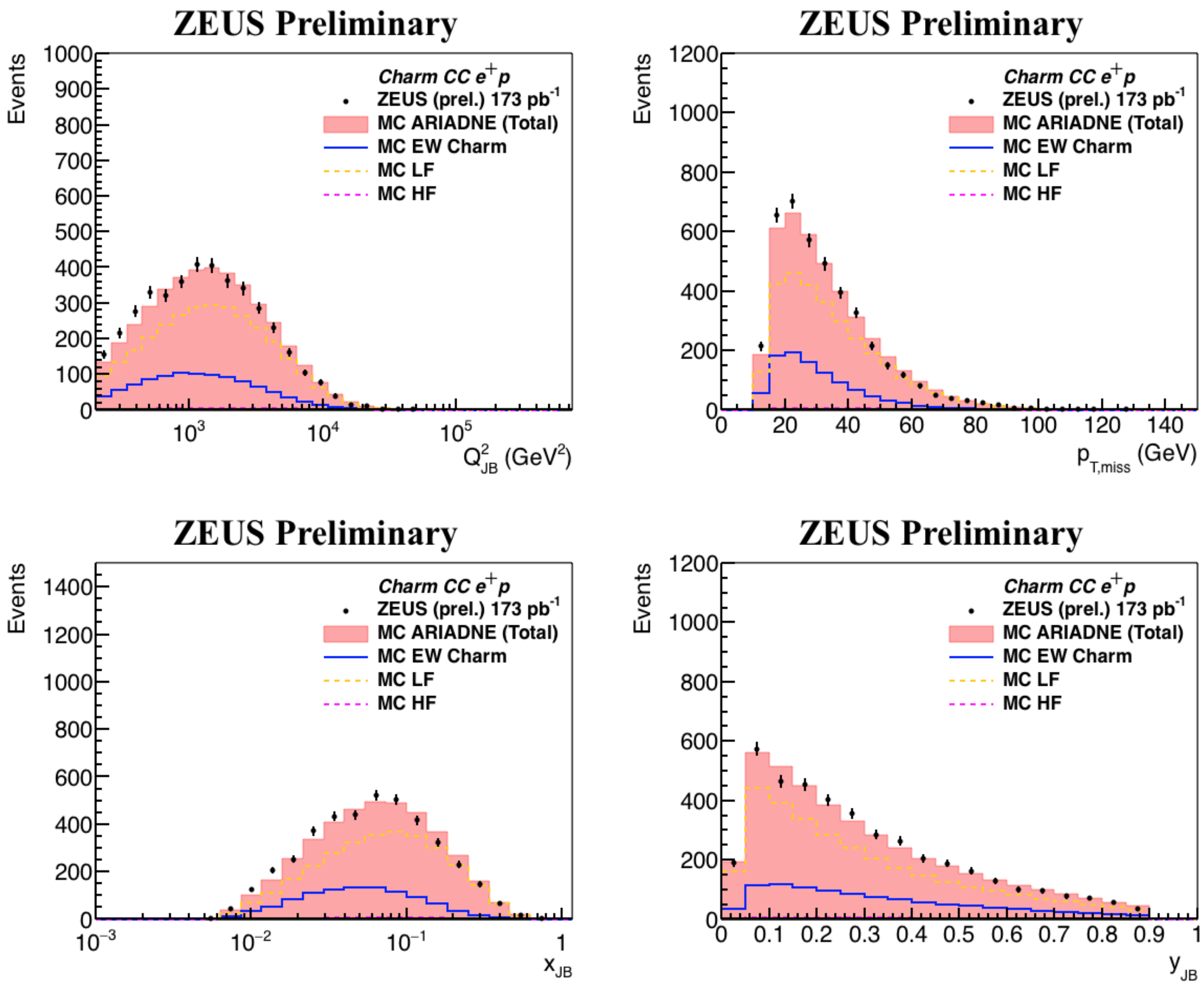

- EW Charm/Anticharm

  Charm from electroweak reaction either in the initial or final state.
- LF

  Light-flavor contribution. Major source of background
- HF

  Heavy Flavor events that do not involve EW charm

B – Cross section unfolding procedure

$$\sigma_{i,charm,CC} = \frac{M_{i,meas} - M_{i,meas}^{bg}}{M_{i,meas}^{MC}} \sigma_{i,charm,CC}^{MC}$$

- The charm cross section is measured by extrapolating the cross section measured in MC samples with a factor $\frac{M_{meas,i} - M_{meas,i}^{bg}}{M_{meas,i}^{MC}}$.
- Here, M denotes the number of entries in reconstructed Q^2_{JB} distribution.

$$\sigma_{i,charm,CC}^{MC} = \frac{N_{i,charm,CC}^{MC}}{L}$$

- The MC cross section is given by the equation on the left, where N denotes the number of entries in true Q^2 distribution.
- The discrepancy between N and M is found to be in the order of ~1%.

$$\sigma_{charm,CC}^{tot} = C_{ext}\, \sigma_{charm,CC}^{vis}$$

- The total cross section can then be extrapolated via an extrapolation factor $C_{ext} := N_{charm}^{full} / N_{charm}^{kin}$, the ratio of the number of generated charm versus that of visible charm.